

# Tribocharging and the Triboelectric Series

Diana M. Gooding

Boston University, Boston, MA, USA

&

George K. Kaufman

Transylvania University, Lexington, KY, USA

1	Introduction	1
2	Characterization	4
3	Mechanisms of Tribocharging	5
4	Conclusions	12
5	Abbreviations and Acronyms	12
6	Glossary	12
7	Related Articles	12
8	References	12

## 1 INTRODUCTION

Just as a magnet is a material with a magnetic field at its surface, an electret is a material with an electric field at its surface (see *Electrets*).<sup>1,2</sup> Electrets often obtain their charge via contact electrification, the charging of materials brought into contact and separated, with or without rubbing. Discussed in this article are electrets formed by tribocharging (also known as triboelectric charging), a process by which materials contact, rub, and separate, leaving each with a net surface charge (tribo- comes from the Greek τριβος, rubbing).<sup>3–5</sup> This phenomenon is well known but poorly understood. Although known to the ancient Greeks and ubiquitous in industry (e.g., toner particles in gas–solid fluidized beds<sup>6</sup> for xerography<sup>7,8</sup>), there remains disagreement about the mechanisms behind triboelectrification and the chemical identities of the charges.

The most consistent description of how materials charge is their empirical arrangement in the triboelectric series (Figure 1). At the top of this list are materials that have a strong tendency to develop a net positive charge when rubbed against materials lower on the list. At the bottom of the list are materials that have a strong tendency to develop a net negative charge when rubbed against materials higher on the list. Chen *et al.*<sup>12</sup> recently reviewed numerous strategies to control tribocharging using this tendency

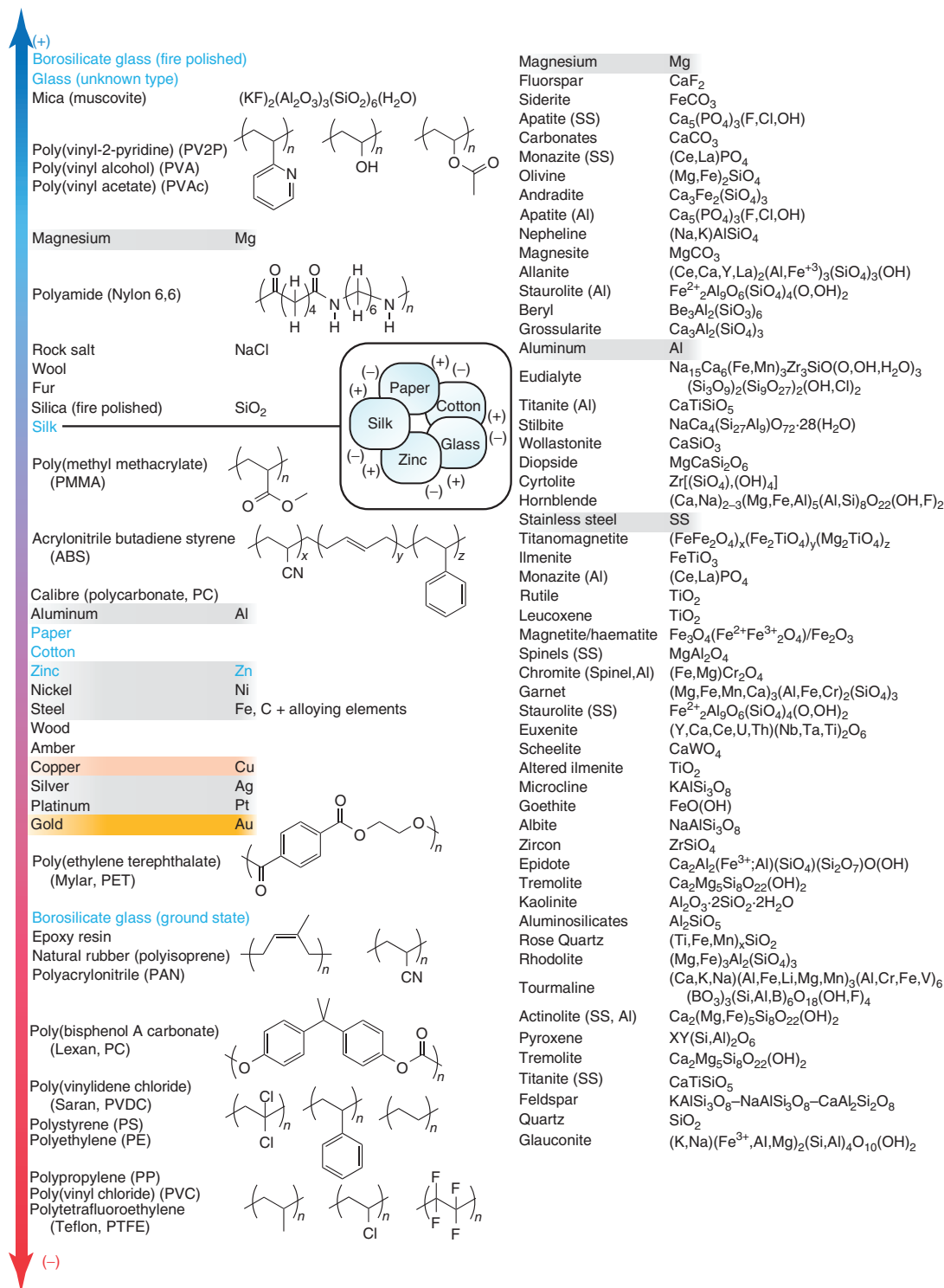
of materials (or chemical functional groups) to charge positively or negatively in the triboelectric series, including copolymerization, surface functionalization with ionic or nonionic molecules, and surface coatings. In general, conductors with low work functions and insulators that are hydrophilic, have high Lewis basicity, and have high donor numbers tend to be nearer the top of the series, where materials tribocharge positively.

One should be cautious, however, when generalizing the specific order of materials with respect to each other in any given triboelectric series. The series for minerals (Figure 1, right) shows various inconsistencies in the specific order. For example, staurolite charges positively against Al but negatively against stainless steel (SS), even though SS also charges negatively against Al. This lack of a consistent, linear order for staurolite, Al, and SS is one of many that are apparent in Figure 1. Likewise, Wiles *et al.*<sup>13</sup> found the opposite order for polystyrene (PS) and polytetrafluoroethylene (PTFE) in their triboelectric series: metal and metal-oxide spheres charged more positively when rolling against PS than they did against PTFE. Their results also suggest that poly(methyl methacrylate) (PMMA) could be significantly higher in the triboelectric series than nylon.

Tables 1–4 give other examples of inconsistent ordering of materials. Charge acquired by *Musca domestica* (houseflies) when walking on the surfaces in Table 1 leads to a generally similar order but different exact order (listed in boldface type) from that found in Figure 1.<sup>14</sup> Water flowing through air or tubes of different materials (Table 2) indicates that water lies near the top of the triboelectric series, between glass and air; the charge developed on water when flowing through these materials forms a quantitative triboelectric series that is also mostly consistent with Figure 1.<sup>15</sup> Copper and steel appear in a different order from Figure 1, but the charges accumulated on water flowing against them are not statistically significant. By shaking pellets in containers made of various materials, Park *et al.*<sup>16</sup> generated a series that was generally similar to that of Figure 1 but had a different order for other materials such as rubber and various types of polystyrene (Table 3). In exploring the distinct contact electrification and separation electrification of insulating polymers with Al, Cu, and SS (Section 3.1), Musa *et al.*<sup>17</sup> generated a quantitative triboelectric series (Table 4) that differs substantially from that in Figure 1. The most pronounced difference was that of PTFE, which charged against Al less negatively than three other materials. PTFE generally charges substantially more negatively than other materials (see Tables 2 and 3).

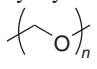
These inconsistencies in the order of the materials in the series can arise when materials are variably strained<sup>18,19</sup> or when different series are produced using different sample preparations (e.g., fire polished or ground borosilicate glass), methods of contact between materials (e.g., impact, rolling, or sliding), and laboratory conditions such as humidity and temperature. There are sometimes large

Update based on the original article by George Kaufman, *Encyclopedia of Inorganic Chemistry* © 2014 John Wiley & Sons, Ltd.



**Figure 1** Triboelectric series of polymers, metals, and inorganic compounds based on semiquantitative data (left)<sup>9</sup> and of minerals based on charging against three different metals (right).<sup>10,11</sup> The order of the series of polymers (left) differs slightly from other sources<sup>1,9</sup> because it reflects the magnitude and polarity of charging with respect to Mg and Al in addition to Au.<sup>9</sup> The series of minerals (right) that charged against stainless steel (SS)<sup>10</sup> and that charged against Al or Mg<sup>11</sup> were combined by minimizing the difference in charging values among the six minerals that were listed in both series. Inset: a cyclic triboelectric series in which the polarity of charge on each pair of materials is listed as positive (+) or negative (-).<sup>1,3</sup> Members of this cyclic series are listed in blue text (left)

**Table 1** A quantitative triboelectric series based on the charging of houseflies walking on various surfaces<sup>14</sup>

Material <sup>(a)</sup>	Contact <sup>(b)</sup> charge (pC)
Acrylic (PMMA)	15 ± 3
<b>Nylon</b>	0.9 ± 1.2
<b>Polycarbonate (PC)</b>	0.4 ± 1.0
<b>Glass</b>	0.4 ± 0.4
Housefly ( <i>Musca domestica</i> )	n/a
Wood (plywood)	−4.1 ± 0.7
Acetal (polyoxymethylene)	−4.7 ± 0.6
(POM) 	
Polyethylene (PE)	−18 ± 1
Polypropylene (PP)	−33 ± 5
Poly(vinyl chloride) (PVC)	−35 ± 4
<b>Correx (corrugated PP), delta insect trap</b>	−54 ± 4

<sup>(a)</sup>Materials that appear in a different order from that in Figure 1 are listed in boldface type.

<sup>(b)</sup>These charges are the opposite of those reported for the charge measured on *Musca domestica*.

**Table 2** A quantitative triboelectric series based on the charging of water after flowing through various materials<sup>15</sup>

Material <sup>(a)</sup>	Charge per mass (pC g <sup>−1</sup> ) <sup>(b)</sup>
Air	15.9 ± 0.9
Water	n/a
Glass	−3.4 ± 0.2
Aluminum	−5.7 ± 0.7
<b>Copper</b>	−26.1 ± 1.1
<b>Stainless steel</b>	−27.9 ± 1.7
Polystyrene (PS)	−50.3 ± 9.9
Silicone	−64.5 ± 1.8
Polytetrafluoroethylene (PTFE)	−198.8 ± 9.8

<sup>(a)</sup>Materials that appear in a different order from that in Figure 1 are listed in boldface type.

<sup>(b)</sup>The opposite of the charge measured on water with standard deviations from five independent experiments.

Source: Reproduced with permission from T. A. L. Burgo, F. Galembeck and G. H. Pollack, *J. Electrostat.*, 2016, 80, 30–33. © Elsevier, 2016.

standard deviations in the charging between materials even when controlling for these variables.<sup>20</sup> For example, quartz (SiO<sub>2</sub>, z-cut (0001)) charges negatively against each of four different sapphire (Al<sub>2</sub>O<sub>3</sub>) orientations: the C-plane (0001), A-plane (1120), R-plane (1102), and M-plane (1100).<sup>21</sup> Despite controlling actuation down to the micrometer level and operating in vacuum, the spread in their charging data for each face was larger than the differences in charging for the different faces. Surface roughness at the nanometer scale could explain this lack of control over charging.<sup>21</sup>

The reversal of charge polarity, in which members of the triboelectric series switch places, when some materials

**Table 3** A quantitative triboelectric series based on shaking polymer pellets in containers made of various materials<sup>16</sup>

Material <sup>(a)</sup>	Charge per mass (nC g <sup>−1</sup> )	
	On pellet <sup>(b)</sup>	In container <sup>(c)</sup>
PMMA	16.1	9.6
<b>GPPS</b>	11.9	
ABS	10.3	4.5
Calibre (PC)	8.8	
Copper		2.5
<b>HIPS</b>	5.3	1.8
<b>Rubber</b>	4.1	
PET	2.5	1.2
HDPE	−0.3	−2.0
LDPE	−3.6	
PP		−4.7
HOMOPP	−4.2	
COPP	−5.0	
PVC		−11.3
S-PVC	−8.9	
H-PVC	−14.2	
PTFE		−17.4

<sup>(a)</sup>Materials that appear in a different order from that in Figure 1 are listed in boldface type. Container materials: polytetrafluoroethylene (PTFE), poly(vinyl chloride) (PVC), polypropylene (PP), high-density polyethylene (HDPE), poly(ethylene terephthalate) (PET), Cu, high-impact polystyrene (HIPS), acrylonitrile butadiene styrene (ABS), and polymethylmethacrylate (PMMA). Pellet materials: hard poly(vinyl chloride) (H-PVC), soft poly(vinyl chloride) (S-PVC), co-polypropylene (COPP, propylene–ethylene copolymer), homo-polypropylene (HOMOPP), LDPE, HDPE, PET, Rubber, HIPS, Calibre™ polycarbonate (PC), ABS, general purpose polystyrene (GPPS), and PMMA.

<sup>(b)</sup>The average of charges measured on pellets of this material charged against containers of all materials.

<sup>(c)</sup>The opposite of the average of the charges measured on pellets of all materials charged against a container this material.

Source: Reproduced with permission from C. H. Park, J. K. Park, H. S. Jeon and B. C. Chun, *J. Electrostat.*, 2008, 66, 578–583. © Elsevier, 2008.

contact and separate from each other repeatedly for a long time further complicates the generation of a uniform triboelectric series.<sup>22,23</sup> For example, in a series of single-crystal fluorides bearing polished (100) faces, MgF<sub>2</sub> consistently charged negatively against CaF<sub>2</sub>, LiF, and BaF<sub>2</sub>, but all combinations of the latter three crystals flipped their polarity when they contacted repeatedly (e.g., CaF<sub>2</sub> first charged negatively against BaF<sub>2</sub>, its charge reached a plateau, and then CaF<sub>2</sub> charged positively).<sup>23</sup> The authors posited that these reversals in charge polarity may result from multiple simultaneous and competing mechanisms for charging, such as changes in surface chemistry, material transfer, and partitioning of surface water layers (see Section 3).

There are also cyclic triboelectric series (Figure 1, inset), as in the case of the series containing (+) zinc, silk, paper, cotton, and glass (−). This list is in order of increasingly negative tribocharging, but the order holds for any starting material. For example, (+) paper, cotton, glass, zinc, and

**Table 4** A quantitative triboelectric series based on the contact and separation of insulating polymers with aluminum<sup>17</sup>

Material <sup>(a)</sup>	Charge (nC) <sup>(b)</sup>
Nylon	0.9
Polycarbonate (PC)	0.5
Aluminum	
<b>Acetate (PMMA)</b>	-0.2
<b>Polypropylene (PP)</b>	-0.4
Poly(ethylene terephthalate) (PET)	-0.6
Kapton	-0.7
<b>Polytetrafluoroethylene (PTFE)</b>	-1.2
Polydimethylsiloxane (PDMS)	-1.8
Polysulfone (PSU)	-2.6
Poly(vinyl chloride) (PVC)	-3.2

<sup>(a)</sup>Materials that appear in a different order from that in Figure 1 are listed in boldface type. Kapton is poly(4,4'-oxydiphenylene-pyromellitimide), a type of polyimide developed by DuPont in the late 1960s. Polyimides have a general subunit structure of  $[-R-(C=O)-N(R')-(C=O)-]$ , where R and R' may be different groups. Polysulfone has a general subunit structure of  $[-aryl-SO_2-aryl'-]$ .

<sup>(b)</sup>These charges are measured on materials after contact and separation with aluminum. The noise in the charge measurement was approximately  $\pm 0.1$  nC.

Source: Musa<sup>17</sup>, <https://www.nature.com/articles/s41598-018-20413-1#rightslink>. Licensed under CC BY 4.0.

silk (–) is also a valid order.<sup>1,3</sup> Lastly, these series imply that tribocharging requires two different materials, but recent work has demonstrated tribocharging between two identical materials.<sup>24,25</sup>

Each of these inconsistencies makes understanding the triboelectric series and the mechanisms behind tribocharging a difficult task. The myriad and growing number of uses for electrets, such as triboelectric nanogenerators (TENGs) for energy harvesting and self-powered sensors, triboelectronics such as contact electrification-based field-effect transistors (CE-FETs), self-powered gas filters, and pulses of X-rays that can be used for X-ray fluorescence and X-ray imaging also makes this task important (see *Electrets*).<sup>12,26–28</sup>

## 2 CHARACTERIZATION

The net charge on tribocharged materials is usually measured inductively. A variety of devices exist for inductive charge measurement, including Faraday cups,<sup>29,30</sup> Faraday tubes (Figure 2),<sup>1,31</sup> and single electrodes in different configurations.<sup>13,32–36</sup> These devices measure the total charge on materials or macroscopic regions of charge, but not microscopic or nanoscopic patterns of charge.

Many of the apparent inconsistencies in the triboelectric series arise from the assumption that surfaces charge uniformly when rubbed together. Several experiments have

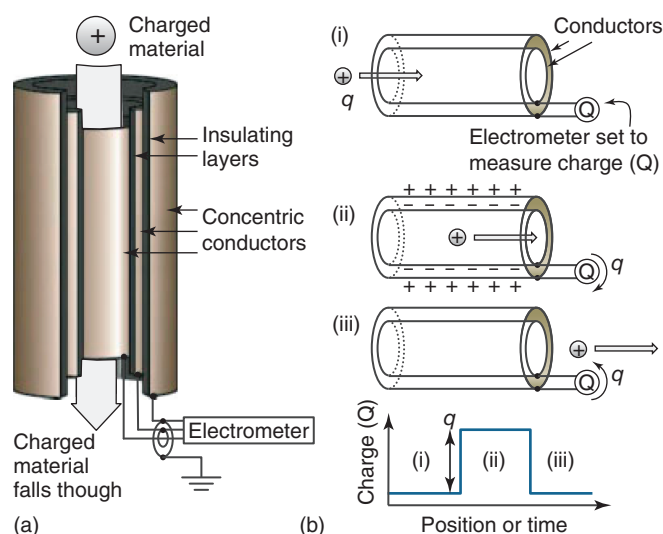


**Figure 2** (a) Schematic representation of a Faraday tube. Portions of the outer two cylinders are removed in this view to show the inner cylinder. An electrometer measures the charge,  $Q$ , between an inner and middle conductor, with respect to a grounded outside conductor. Charged materials can pass through the conductors, or into a set of conducting containers that form a Faraday cup, which has the same three-layered structure. (b) Charge,  $q$ , flows between the inner and middle copper cylinders of the Faraday tube to compensate for the enclosed charge ( $q$ ) on the material. Measuring the charge on the electrometer as a function of time will indicate the value of  $q$

shown that this assumption is not necessarily true, but rather that some surfaces develop microscale or nanoscale mosaics of *both* positive and negative charges.<sup>22,37,38</sup> These positive and negative regions on electret surfaces can be characterized by a variety of surface analytical techniques. Kelvin-probe atomic force microscopy (KFM) can finely probe, map, and quantify charge at submicrometer length scales, and magnetic force microscopy (MFM) can visualize the microscopic distribution of radicals. The measurement of triboluminescence (the production of X-ray, visible, and RF emissions) can probe the transient, microscale processes that occur during triboelectrification and their relationship to triboplasma.<sup>21,28,39</sup> Measuring open-circuit electrical potential and current (e.g., with an oscilloscope and current preamplifier) can probe the electrostatic induction and transfer of charge during the distinct contact and separation steps of contact electrification.<sup>17</sup> Infrared (IR), Raman, and nuclear magnetic resonance (NMR) spectroscopies can aid in chemical identification. Electron spin resonance (ESR), also known as electron paramagnetic resonance (EPR), can analyze trapped charged radical and paramagnetic species. One of the most frequently used techniques to characterize the surfaces of dielectric electrets is X-ray photoelectron spectroscopy (XPS), which can determine the atomic composition, and in some cases the chemical identity, of the surface of a material.<sup>40</sup>



### 3 MECHANISMS OF TRIBOCHARGING

#### 3.1 Overview of Mechanisms

If one particular property (e.g., dielectric constant or work function) determined the charging of all materials, then they would fit into a unique, consistent, and self-consistent triboelectric series. However, some materials fall into cyclic series (Figure 1)<sup>1,3</sup> and other pairs of materials reverse the polarity with which they charge when repeatedly tribocharged against each other (probably because of material transfer)<sup>22</sup> or when one of the materials (e.g., latex rubber) is variably strained.<sup>18</sup> Apodaca *et al.*<sup>24</sup> observed the tribocharging of identical materials of the same size, and several other groups noticed that smaller particles generally charge negatively against larger particles of identical composition<sup>41,42</sup>—processes that should not happen because the chemical potentials of the materials are identical, especially when materials of the same size and shape are brought together symmetrically. Wang *et al.*<sup>25</sup> demonstrated that differences in the microstructure (e.g., the presence of voids and crazes) but not the molecular-scale structure in otherwise identical materials led to charge transfer during contact: PTFE with 100% strain charged positively against PTFE with 0% strain, whereas charge transfer was relatively small in magnitude and random between PTFE samples with the same (0% or 100%) strain. These charging behaviors that appear to be inconsistent with a unique triboelectric series have, in part, motivated current research on the mechanisms and charge-carrying species present during tribocharging. These observations also suggest that more than one property or mechanism contributes to charging.

Mechanisms for tribocharging and control of charging have been recently reviewed, including important parameters and environmental factors such as charge injection depth, dielectric breakdown of materials and the atmosphere, surface capacitance, surface charge density, surface microstructure, particle size, load stress, humidity and acidity, and external electric fields.<sup>12,43,44</sup> Pan and Zhang<sup>43</sup> also reviewed theoretical descriptions for these factors. Temperature also affects tribocharging.<sup>45–48</sup> Charges may form as electron–hole pairs or via various processes such as separation of ions, heterolytic bond dissociation, or homolytic bond dissociation followed by oxidation or reduction reactions with atmospheric gases. Charge transfer then generally takes place via one or more of three broad categories: electron transfer (Section 3.2),<sup>3,8,49–54</sup> ion transfer (Section 3.3),<sup>1,9,31,34,53,55</sup> and bond breaking followed by material transfer (Section 3.4).<sup>22,37,38,56–60</sup>

Importantly, these charges may form, transfer, and dissipate differently in the distinct contact and separation steps of tribocharging. For example, during the contact and separation of an insulating polymer with either a metal or a second insulating polymer,<sup>17</sup> contact is characterized

by three electrical steps: (i) electrostatic induction if the two materials are charged prior to contact, and (ii–iii) two *oppositely* charging processes (a “bipolar” charging process, + followed by – or – followed by +) on *each* material. Musa *et al.*<sup>17</sup> argued that this temporally resolved bipolar contact charging requires spatial bipolar charging (the formation of both + and – charges) on the polymer surface. Separation is then characterized by two sequential but temporally overlapping electrical steps: (i) a single “unipolar” (+ or –) charging process, and (ii) electrostatic induction. Thus, understanding the mechanisms of tribocharging, and the relative contributions of electron, ion, and material transfer, may require techniques with temporal resolution that can separately investigate these steps.

Electrons appear to tunnel between metals according to the difference in their work functions,<sup>3,8</sup> but electron transfer does not, in theory, easily extend to insulators.<sup>1,9,56</sup> Electron transfer from nylon to polyethylene (PE), consistent with the polarity predicted by the triboelectric series, is endothermic by 5–10 eV, a few orders of magnitude higher than thermal energy at room temperature ( $k_B T \approx 0.026$  eV).<sup>1</sup> Most experiments also appear to refute electron transfer when one or each member of the tribo-pair is an insulator, for which tribocharging does not correlate with bulk electronic properties such as work function and dielectric constant or with atomic properties such as ionization energy, electron affinity, and electronegativity.<sup>1,61</sup> Charge transfers between contacting insulators even when they lack the well-matched, electron-rich donor and electron-poor acceptor orbitals found in the functional groups of known charge-transfer complexes. Doping polymers with these electron-rich molecules does not affect their tribocharging.<sup>9</sup> Liu and Bard hypothesize that there may be high-energy “cryptoelectrons” that transfer between insulating materials and that these electrons are responsible for a range of reduction reactions that can occur at negatively tribocharged surfaces,<sup>49–52</sup> but Lubomirsky and coworkers suggest that these observations stem from material transfer followed by adsorption of ions to polar groups on the surfaces but not reduction of those ions,<sup>57,58</sup> and Baytekin *et al.* and Yun *et al.* assert that such reactions are driven by the formation of mechanoradicals.<sup>56,62,63</sup>

The transfer of ions or radicals thus appears to be responsible for tribocharging between insulators. As humidity plays a role in tribocharging,<sup>32,33,43,64–69</sup> proton transfer is a possible related mechanism.<sup>3,9</sup> Exposure of charged surfaces to water-soaked hydrogels can dissipate the charge on these surfaces faster than the decay of this charge in air.<sup>70</sup> Baytekin *et al.*<sup>69</sup> found, however, that water can help to stabilize the charges that develop on surfaces and that tribocharging can also occur in the complete absence of water. Because zero humidity limits but does not eliminate tribocharging, proton transfer or

partitioning of  $H^+$  and  $OH^-$  from water layers or the atmosphere may contribute to tribocharging but cannot be the sole mechanism.

In some cases, there is a correlation between tribocharging and Lewis acidity or basicity,<sup>9</sup> with acidic substances tending to charge negatively and basic substances tending to charge positively. Figure 1 shows several basic compounds—poly(vinyl-2-pyridine) (PV2P), carbonates and phosphates—or those with high donor number near the top of the triboelectric series, where compounds charge positively, and more acidic compounds near the bottom. Despite this correlation, one cannot accurately infer whether electron or ion transfer is behind tribocharging. Because the Lewis acid–base definition only implies that an acid and base share an electron pair, it does not imply the extent to which chemicals oxidize or reduce (e.g., the 3d metal cations are Lewis acids and powerful reductants).<sup>1</sup> Moreover, oxidation–reduction properties of certain organic dopants do not correlate with the triboelectric series of materials containing them. Instead, it is likely that a correlation between Lewis acidity and tribocharging may be related to the transfer or partitioning of ions (e.g.,  $H^+$  or  $OH^-$  from the atmosphere or from thin layers of water adsorbed on the surface of the materials) between the tribocharged substances.<sup>9</sup> It is possible that such a mechanism for tribocharging is related to hygro-electricity, the humidity-dependent buildup of charge on a surface, where acidic surfaces develop a negative charge and basic surfaces develop a positive charge when exposed to increased humidity.<sup>64,71</sup>

One reason why most bulk properties do not appear to correlate with the polarity and magnitude of tribocharging is that most studies to date have not accounted for material transfer between surfaces (Section 3.4).<sup>22,37,56–59</sup> Material transfer can contribute to the reversal of charge polarity during tribocharging.<sup>22</sup> For example, characterization of the surfaces of PTFE spheres and PS dishes that had tribocharged against one another showed that fragments of one material had transferred to the surface of the other. These fragments resulted in “mosaics” of positive and negative charges on *both* surfaces, rather than a homogenous charge across each tribocharged surface, as previously thought.<sup>22,37</sup> Surface charges appear to colocalize with radicals and correspond to regions in which material has transferred from one member of the tribopair to the other.<sup>59</sup> The observation that charge can transfer between identical materials further demonstrates that tribocharging may be driven by molecular-scale changes in the surface chemistry of insulators.<sup>24,25</sup> Therefore, mechanical and chemical properties such as relative hardness or softness and cohesive energy of a material may be just as important to tribocharging as bulk electronic properties.<sup>22</sup>

## 3.2 Electron Transfer

### 3.2.1 Metal–Metal Charging

Some of the earliest research on the triboelectric series involves determining the role of electrons in the tribocharging of metals, which is fairly well-understood<sup>1,9</sup> and contributes to the coupled electrical and mechanical phenomena behind friction and wear for contacting metals.<sup>53</sup> Pai and Springett<sup>8</sup> summarize this phenomenon nicely: electrons tunnel from the metal of lower work function to the metal of higher work function until the Fermi levels of the metals coincide (Figure 3). Tribologically introduced phonon–electron interactions provide the driving force for electron transfer.<sup>54</sup>

For metals A and B, with work functions  $\Phi_A$  and  $\Phi_B$ , a contact potential difference  $V_c$  exists between them at thermodynamic equilibrium (Equation 1, in which  $e$  is the charge on an electron).

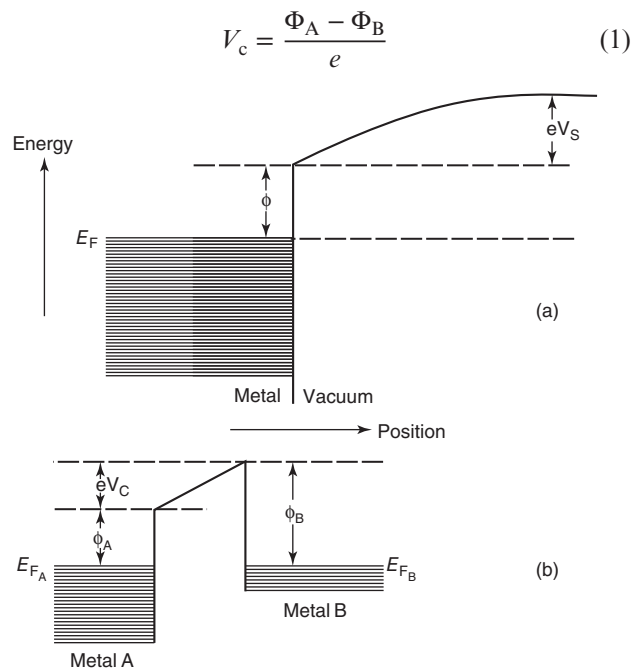


**Figure 3** A difference in contact potential ( $V_c$ ) appears to determine the tribocharging of metals and possibly other conductive materials. (a) The work function ( $\Phi$ ) is the energy required to remove an electron from a material to a point immediately outside its surface. The work function is related to the Fermi level ( $E_F$ ), the thermodynamic energy required to add an electron to the material. The surface potential ( $V_s$ ) is the energy required to move an electron from the surface to infinite distance. (b) When two metals (A and B) contact each other, electrons transfer until the Fermi levels ( $E_{FA}$  and  $E_{FB}$ ) are equal and the two metals are in thermodynamic equilibrium. This charge transfer creates a contact potential difference equal to the difference between the work functions of the two metals ( $\Phi_A$  and  $\Phi_B$ ). [Reproduced with permission from Ref. 8. Copyright (1993) by The American Physical Society]

Theoretically, the charge ( $Q$ ) transferred between these metals should be the product of this potential difference and the effective capacitance ( $C$ ) between them (Equation 2).

$$Q = CV_c \quad (2)$$

Table 5 gives the contact potentials relative to chromium for a range of metals, oxides, and sulfides, as well as the charge on several metals after contacting a chromium sphere.<sup>3</sup> These charges agree with theoretical predictions based on tunneling of electrons (Equation 2) for the case of  $C$  being the capacitance between a 5/32-inch sphere (Cr) and a 1/2-inch sphere (other metal) separated by a distance of 1 nm.<sup>3,8</sup> (As this tunneling current weakens at ~1 nm, the quantity of charge transferred between these metals is the product of their contact potential difference and their capacitance at 1-nm spacing.) One explanation for slight discrepancies between the theoretical and observed charges is that the surfaces of the metals are not perfectly smooth or spherical at the nanometer scale.<sup>3,8</sup> It is important to note that the work function based on the photoelectric effect<sup>72</sup> does not always coincide with the contact potential of that material. The largest departure appears to be that for zinc. This difference suggests that the mechanism of contact charging of some materials, even metals, may involve more than just electron transfer. For example, tribocharging among metals and other conductive materials could involve the partitioning of  $H^+$  and  $OH^-$  ions found in the thin layer of water that coats each surface.

### 3.2.2 Metal–Insulator Charging

Inconsistent laboratory conditions<sup>8,68</sup> and poorly characterized surface states of polymers<sup>41</sup> often hamper progress on understanding metal–insulator charging. Wiles *et al.* developed a rolling-sphere tool which they<sup>13,33</sup> and others<sup>34,35,68</sup> have used to collect reproducible charging data between metals and solid insulators (Figure 4). Using this tool, charge on a metal sphere rolling on a polymer surface grows sigmoidally in time, indicating that each polymer surface investigated has a charge saturation point. Grzybowski *et al.*<sup>68</sup> claimed that saturation occurs when electrons tunnel from the metal to the polymer surface and raise the characteristic energy level of the polymer above the Fermi level of the metal. Musa *et al.*<sup>17</sup> proposed that during metal–insulator contact charging there is bipolar charge creation (e.g., formation of  $X^+$  and  $Y^-$  mechanoions and free electrons,  $e^-$ ), followed by the flow of these free electrons within the metal. See *Electrets* for electrode–liquid charging.

Lu *et al.*,<sup>45</sup> Su *et al.*,<sup>46</sup> and Wen *et al.*<sup>47</sup> studied the temperature dependence of the electrical performance of triboelectric generators (TEGs)<sup>47</sup> and TENGs<sup>45,46</sup> that operated based on contact electrification between Al and PTFE. For Lu *et al.*, the open-circuit voltage and short-circuit current of their device either decreased or remained relatively stable from  $-20^\circ\text{C}$  to  $150^\circ\text{C}$ . They attributed this change in performance to two factors. First, a decrease in the relative permittivity (dielectric constant) of the PTFE, and thus a decreased ability of the PTFE to store charge, matched the decrease in electrical performance of the device. Second, XPS and IR spectra showed

**Table 5** Triboelectric series based on contact charge<sup>3</sup> or contact potential<sup>11</sup> of metals, oxides, and sulfides

Material	Contact charge (pC)	Contact <sup>(a),(b)</sup> potential (V)	$\Phi^{(b),(c)}$ (eV)
Magnesium	Mg	0.85	3.66
Aluminum	Al	0.49	4.17
Zinc sulfide	ZnS	0.09	
Chromium	Cr	0	4.50
Cobalt	Co	−0.19	<b>5.00</b>
Zinc	Zn	−0.30	<b>3.63</b>
Nickel	Ni	−0.34	<b>5.20</b>
Steel	SS	−0.36	4.63
Copper	Cu	−0.37	<b>4.76</b>
Silver	Ag	−0.45	4.63
Rhodium	Rh	−0.52	4.98
Platinum	Pt	−0.56	<b>5.53</b>
Copper sulfide	CuS	−0.68	
Silver sulfide	Ag <sub>2</sub> S	−0.70	
Gold	Au	−0.75	5.38
Lead(IV) oxide	PbO <sub>2</sub>	−1.57	

<sup>(a)</sup>Contact potential relative to chromium,<sup>3</sup> except for Mg, Al, ZnS, CuS, Ag<sub>2</sub>S, and PbO<sub>2</sub> (relative to Ni)<sup>11</sup> and Zn, which is estimated from the contact potential listed in the CRC Handbook of Chemistry and Physics.<sup>72</sup>

<sup>(b)</sup>Bold values are out of order compared to charging.

<sup>(c)</sup>Work function from the photoelectric effect. Numbers are for polycrystalline samples, if listed. Otherwise, this number is an average for the work function for all crystal faces.<sup>72</sup>



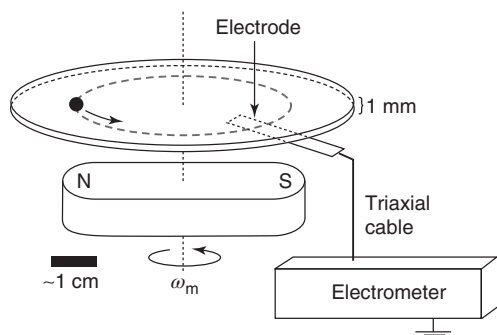


**Figure 4** Illustration of a rolling-sphere tool used to study the polarity, magnitude, and kinetics of tribocharging between magnetic spheres (coated or uncoated) and planar insulating surfaces, here shown as a 1-mm thick wafer.<sup>34</sup> The electrode (connected to an electrometer) capacitively measures the charge on the surface and the sphere as a rotating magnet (usually a magnetic stir plate) causes the sphere to roll. When the sphere is far from the electrode, the electrometer reports only the charge on the portion of the surface to which the electrode is coupled. When the sphere is near or directly above the electrode, the electrometer reports the sum of the charges that the electrode senses on the sphere and the surface.<sup>35</sup> Puhan, *et al.*<sup>39</sup> used a modified version of this tool to measure triboluminescence from corona discharge. They replaced the rolling sphere with a camera, spectrometer, and sapphire (single crystal alumina,  $\text{Al}_2\text{O}_3$ ) hemisphere, which slid as the insulating surface rotated beneath it. [Reproduced with permission from Ref. 34. Copyright 2008 WILEY-VCH Verlag GmbH & Co. KGaA, Weinheim]

that the PTFE reacted more with atmospheric oxygen at elevated temperatures, replacing surface F atoms with O atoms. They concluded that these reactions decreased the effective electron trap density on the PTFE.<sup>45</sup> Su *et al.*<sup>46</sup> noticed a similar decrease in the output voltage and current over a temperature range of  $-196^\circ\text{C}$  to  $47^\circ\text{C}$  (77–320 K). Wen *et al.*<sup>47</sup> noticed a generally decreasing output voltage and current over the range of  $-196^\circ\text{C}$  to  $227^\circ\text{C}$  (77–500 K) that peaked strongly near  $-13^\circ\text{C}$ . They attributed this peak to an increase in the ductility and softness of the PTFE, which should increase friction and tribocharging, competing with an increase in thermal fluctuations and thus increase in backward electron transfer from the PTFE to Al, which would decrease tribocharging, at higher temperatures. Olsen *et al.*<sup>48</sup> were able to describe these results<sup>45–47</sup> (except for the peak in performance<sup>47</sup>) using a two-level Schottky model for ion transfer, so it is not clear whether the charging mechanism for these systems involved electron transfer or ion transfer. It is also interesting to note that TENGs based on contact electrification between PTFE and  $\text{TiO}_2$  nanotubes or Al-coated  $\text{TiO}_2$  nanotubes both *increased* in electrical performance with increasing temperature,<sup>46</sup> behavior that could not be modeled with a simple two-level Schottky model.<sup>48</sup>

Williams studied the charge penetration depth (CPD) of several insulators when tribocharged against bare metal

or other insulators.<sup>73</sup> Williams examined four systems of varying bulk and surface compositions, polymer films of which the surface layer and bulk had markedly different tribocharging properties (e.g., PVC films containing Vulcan 3 carbon black). This PVC–carbon black film charged by cascading 100- $\mu\text{m}$  beads of bare nickel, bare steel, and steel coated with an insulating layer of styrene/methyl methacrylate copolymer. Insulator–metal tribocharging depended on the composition of the bulk, but insulator–insulator tribocharging did not. Williams hypothesized that the carbon black particles were covered by a layer of polymer thicker than the CPD of the film and that tribocharging occurred via both electron- and ion-transfer for metal–insulator charging. Because the tribocharging between insulators affects only the surface, the tunneling of electrons is less likely than the transfer of ions.<sup>73</sup>

### 3.2.3 Insulator–Insulator Charging

A model for tribocharging based on the tunneling of electrons breaks down when applied to insulators. Density functional theory calculations of the highest- and lowest-occupied molecular orbitals and Fermi levels of various insulating materials suggest that electron transfer may be consistent with their observed tribocharging.<sup>74</sup> Tribocharging of insulators does not, however, correlate with bulk electronic properties such as dielectric constant or with atomic properties such as ionization energy, electron affinity, or electronegativity.<sup>1</sup> This and the work by Williams described earlier suggest that tribocharging of insulators is not a bulk phenomenon caused by tunneling electrons.<sup>73</sup> Liu and Bard<sup>49–52</sup> and Ma *et al.*<sup>70</sup> observed a variety of chemical reduction reactions on the surfaces of PTFE,<sup>49</sup> PMMA,<sup>50,70</sup> and PE (see *Electrets*).<sup>52</sup> They argued that these reactions were evidence that electron transfer is responsible for tribocharging between insulators; however, Lubomirsky and coworkers,<sup>57,58</sup> Baytekin *et al.*,<sup>56,62</sup> and Yun *et al.*<sup>63</sup> attribute these reactions to the formation of mechanoradicals, material transfer, adsorption (but not reduction) of ions to polar groups on the insulating surfaces, and reduction of ions by the mechanoradical species (Section 3.4). Thus, it is still uncertain whether electrons can be responsible for insulator–insulator tribocharging.

## 3.3 Ion Transfer

Evidence for tribocharging via ion transfer comes in part from metal–metal charging, where both electrons and metal ions can act as charge carriers,<sup>53</sup> and electrophotography, where the materials involved contain mobile ions.<sup>3,7,8</sup> In the latter process, either (i) a plasma or corona discharge charges a photoconductive imaging drum, or (ii) an imaging powder (toner particles) tribocharges against insulating carrier beads or a cylindrical



roller and blade.<sup>8</sup> Development of this process required “charge-control agents” to produce toners that would charge more reliably. Electron donors, such as aromatic compounds, and electron acceptors, such as quinones, are ineffective charge-control agents, whereas ionic organic dyes are the most successful. Of these organic dyes, those that contain a bulky organic cation and a mobile anion produce positively charged toners, and those that contain a bulky organic anion and a mobile cation produce negatively charged toners.<sup>75</sup> These observations indicate that, at least in this system, the charge carriers are mobile ions, rather than free electrons. McCarty and Whitesides ruled out other mechanisms for this system, such as oxidation, by comparing the oxidation potentials of the dyes with their effect on tribocharging; the absence of correlation between the two implies that electron transfer is not responsible for the charge these toners develop.<sup>1,75</sup>

For the charging between metals and insulating polymers, somewhat linear trends exist (i) between  $\log(q+1)$  and the  $pK_b$  of molecular analogs for the polymers, where  $q$  is the charge transferred, and (ii) between  $\log(q)$  and the donor number (DN) of the molecular analogs for the polymers.<sup>9</sup> The correlation with  $pK_b$  suggests that the charge transferred may be protons from the dissociation of water molecules adsorbed on the surfaces of the materials. The correlation with DN suggests that polymer–metal tribocharging may result from the transfer of metal cations to the polymer.

The most compelling evidence for transfer of mobile ions comes from studies of acidic and basic ion-exchange resins<sup>76</sup> and polymers that contain covalently bound ions and mobile counterions (Figure 5).<sup>1,31,34,35,55,77</sup> The sign of the charge evolved on these polymers after tribocharging is equal to the sign of its bound ion. Doping such a polymer with more ions leads to increased charging, and XPS demonstrates transfer of only the mobile ion.<sup>78</sup> McCarty *et al.*<sup>31</sup> further corroborated these observations by measuring the charge on functionalized polystyrene or glass microspheres after contact electrification with aluminum. Some of the beads were functionalized with a bound cation and mobile anion, some with a bound anion and mobile cation, and some patterned with different functional groups in different locations. Each bead charged with the same polarity as its bound ion. Beads functionalized with equal amounts (hemispheres) of bound cations and anions developed almost no charge. McCarty and Whitesides proposed the following mechanism for tribocharging via mobile-ion transfer: (i) the mobile ion begins in a single potential well when the materials are contacting; (ii) as the materials separate, the potential splits into two wells, one for each surface; and (iii) the mobile ion overcomes the energy barrier between the two wells by the mechanical work done to separate the surfaces.<sup>1</sup>

Important to this and other treatments of mobile ions in ambient conditions<sup>1,79</sup> is consideration of two competing

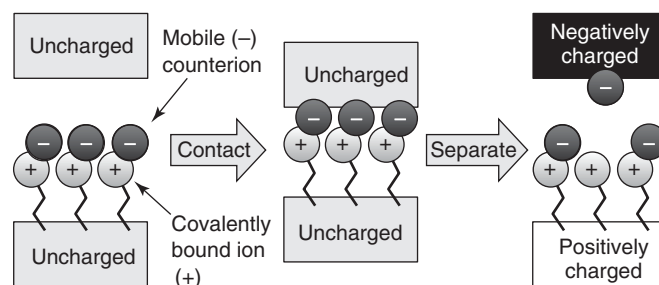


**Figure 5** Hypothetical mechanism for tribocharging by ion transfer. A surface that bears covalently bound ions (shown here as cations) and mobile counterions (shown here as anions) contacts another surface, which could be an insulator or conductor, and some of the mobile counterions transfer between the surfaces before or after they separate

tendencies: entropy and electrostatics. Consider two planar, equally and oppositely charged surfaces, at a spacing of  $d$  nanometers, with  $N$  ionic functional groups per unit area. Under thermal equilibrium, a constant electric field and thus charge density exists between them, and  $n$ , the number of anions per unit area on each surface is given by the Boltzmann distribution (Equation 3), in which  $\epsilon_0$  is the permittivity of free space,  $k_B$  the Boltzmann constant, and  $T$  the temperature (K).<sup>1</sup>

$$\frac{n}{N-n} = \exp\left(-\frac{nde^2}{\epsilon_0 k_B T}\right) \quad (3)$$

Although entropy would have the same number of mobile ions populate each surface, electrostatics tends to join opposite charges. When the surfaces are close enough, the amount of charge evolved on each is limited by discharging events that occur via tunneling, field emission, or the dielectric breakdown of air.<sup>1,3,8</sup>

If the charge density on these surfaces is constant, and the surfaces are flat parallel planes, the electric field between them is also constant and proportional only to the charge density. As the surfaces separate, the potential difference between them increases (Equation 4).

$$E = \Delta V/d \quad (4)$$

When the spacing is  $<2$  nm, electrons can tunnel to the positively charged material. Beyond this distance, the probability of tunneling diminishes drastically (Figure 6a). For large electric fields ( $>5 \times 10^4$  kV cm<sup>-1</sup>), the potential gradient is so steeply sloped that electrons can tunnel, via field emission, into vacuum (Figure 6b). In the dielectric breakdown of the gas surrounding the system (Figure 6c), gaseous species—ionized by ambient radiation or by the strong electric field between the surfaces—and electrons are accelerated by the electric field, collide with other gaseous particles and ionize them, creating a conductive pathway

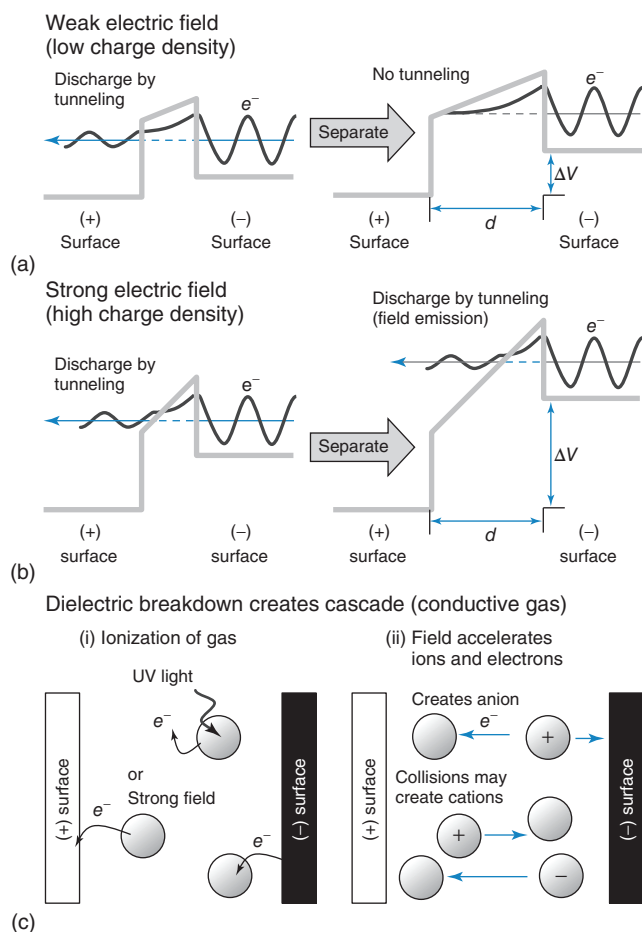


**Figure 6** Mechanisms of discharge that limit the charge on surfaces. (a) A weak electric field (less than  $\sim 10^4$  kV cm $^{-1}$ ) between oppositely charged surfaces allows electrons to tunnel between surfaces at small separations but not at large separations ( $>1$ – $2$  nm). (b) A strong electric field allows electrons to tunnel between two oppositely charged surfaces, including at large distances by field emission. (c) Illustration of dielectric breakdown of air, in which a cascade of ions forms a conductive path between oppositely charged surfaces. [Modified with permission from Ref. 1. Copyright 2008 WILEY-VCH Verlag GmbH & Co. KGaA, Weinheim]

of gaseous ions between the surfaces. Because the dielectric breakdown of air occurs at  $\sim 30$  kV cm $^{-1}$ , this discharging process can effect a surface with a charge density of  $\sim 300$  elementary charges per square micrometer, a common net charge density for tribocharged polymers.<sup>1,3</sup>

### 3.4 Material Transfer and the Formation of Mechanoradicals

Although McCarty and Whitesides presented a convincing argument for an ion-transfer mechanism for ionic polymers,<sup>1</sup> their work left open the identity of charge carriers in nonionic insulators such as PE, PTFE, or

SiO<sub>2</sub>. Commenting on the lowered molecular weights of calendered polymers, Henniker suggested in 1962 that these charge carriers could be high energy electrons liberated from free radicals formed during mechanical stress.<sup>80</sup> Research on the identity of charge-carrying species between tribocharged insulators, then, has focused on detecting these radical species and the ions and oxides they readily form.<sup>38,56,57</sup>

The contact and separation of materials may lead to the formation of ions via heterolytic bond dissociation or the formation of radicals (mechanoradicals) via homolytic bond dissociation. These ions and radicals may then transfer between materials during tribocharging. The amount of material transfer (material wear rate) linked to tribocharging appears to depend exponentially on the physical, normal load stress on the system.<sup>43</sup> There are three main lines of evidence for such material transfer: (i) XPS, which can track the presence of atoms or molecules that transfer from one member of the tribopair to the other; (ii) patterned charge on metal surfaces brought into contact with patterned insulators; and (iii) a heterogeneous charge distribution on each member of the tribopair.

#### 3.4.1 X-Ray Photoelectron Spectroscopy and Patterned Charges on Metals

XPS has shown that material transfer appears to depend on the relative hardness and cohesive energy of the tribocharging materials. Pandley *et al.*<sup>60</sup> observed that soft polydimethylsiloxane (PDMS, a silicone elastomer that can be prepared with varying elasticity and hardness) transfers more material and more electrostatic charge upon contact with PVC than does hard PDMS, as demonstrated by an increase in surface roughness and the presence of silicon atoms (Si 2p peaks) on the PVC after contact. Similarly, Baytekin *et al.*<sup>22</sup> used XPS to observe material transfer from PTFE and PVC (which are relatively soft) onto PS (which is relatively hard) and subsequent polarity reversal of charging. They observed no material transfer and no polarity reversal between cellulose acetate, PMMA, and PS (all relatively hard), and no material transfer between nylon and PS. Nylon is relatively soft, but it has a high cohesive energy, which means that there is a large energy barrier to separate polymer chains from its surface. Sayfidinov *et al.*<sup>81</sup> investigated cellulose tribocharged against PTFE and observed an increase in the oxidation of the cellulose as well as the presence of fluorine (a large F 1s peak and a small C-F signal) on the cellulose after sliding PTFE against the cellulose.

Yun *et al.*<sup>63</sup> formed patterns of positive charge on Au surfaces brought into contact with patterned PDMS. After separation of the Au and PDMS, the positive charge would spread across the Au to form an equipotential surface in the case of electron transfer from Au to PDMS. Instead, the fact that the charged regions of the Au surface remained

localized at the points of contact between the Au and PDMS suggested that material, with charges bound to molecular orbitals, transferred from the PDMS to Au.

### 3.4.2 Heterogeneous Charge Distribution

The expression  $nde^2/\epsilon_0$  in Equation (3) assumes that there is a uniform distribution of charge on each surface. Such a uniform charge distribution has been observed on metal surfaces,<sup>82</sup> but several groups have shown that the charge distribution on tribocharged insulating (e.g., polymer or glass) surfaces exists as a nonuniform mosaic of nanoscale or microscale charged regions of both positive and negative polarity.<sup>37,38,82</sup> Musa *et al.*<sup>17</sup> observed temporal bipolar charging (+ then – or – then +) during metal–insulator and insulator–insulator contact and argued that such temporal bipolar charging required bipolar (both + and –) spatial charging—that is, the formation of charge mosaics. These studies involved materials that did not bear explicit mobile ions as depicted in Figure 4, although the reactive mechanoradicals they propose to be responsible for material transfer during tribocharging could ionize under their experimental conditions.<sup>37,38</sup> These mosaics may have charge densities of  $\sim 1$  elementary charge per  $10\text{ nm}^2$  ( $\sim 1\text{ }\mu\text{C cm}^{-2}$ ) or  $\sim 100\,000$  elementary charges per square micrometer. Thus, the actual density of charges on tribocharged surfaces may be three orders of magnitude larger than the net charges observed on these surfaces would indicate.

Irregularities in the charge landscape arise together with an increased surface roughness and thus a poorly controlled amount and location of material transfer. Baytekin *et al.* challenged<sup>22,37</sup> the long-held view that tribocharged surfaces charge uniformly and that the characteristics of this charging are related to macroscopic (not molecular) properties.<sup>3,4,20</sup> They hypothesized that, rather than a homogenous surface of charge-donating or charge-accepting parts, each surface contains a random mosaic of these parts that overlap during contact.<sup>37</sup> Characterizing these patterns of charge using confocal Raman spectroscopy and XPS revealed changes in the composition of each material, particularly an increase in the intensity of signals assigned as oxidized species: carbonyls and carboxy or peroxy acids. These results, along with previous work on the degradation of elastomers and their subsequent formation of oxidized species after homolytic and heterolytic bond dissociations, suggest that these charge mosaics arise from bond cleavage, redox reactions, and material transfer (Figure 7).

More experimental evidence for this mechanism comes from work by Burgo *et al.*<sup>38</sup> on a familiar tribopair, PE and PTFE. Characterization of these tribocharged surfaces with electron-energy loss spectral imaging, IR microspectrophotometry, and carbonization/colorimetry revealed fluorocarbanions and hydrocarbocations on each

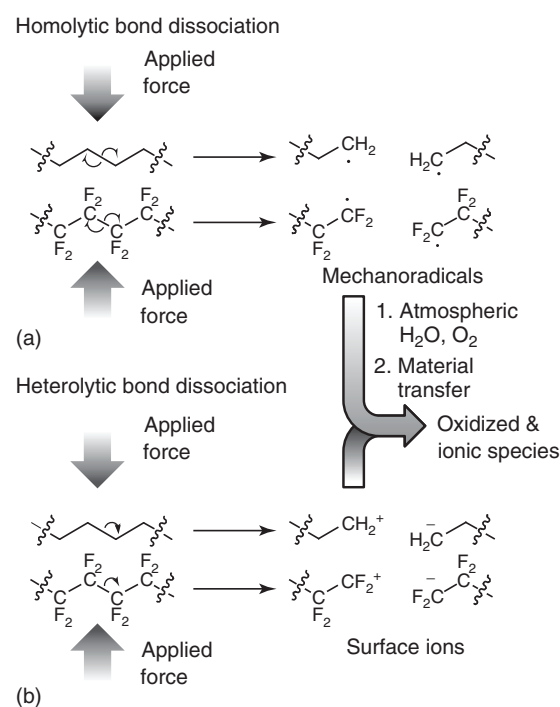


**Figure 7** Schematic representation of (a) homolytic bond dissociation that may result in the formation of mechanoradicals and (b) heterolytic bond dissociation that may result in ions produced at the surface of two materials (PTFE and PE are shown here) during tribocharging. Atmospheric water and/or oxygen may react with these reactive species. Subsequent material transfer has been inferred from IR reflectance spectra,<sup>38</sup> confocal Raman microscopy and XPS<sup>22,37</sup>

surface. Their mechanism is slightly different but not entirely inconsistent with what Baytekin *et al.* describe: mechanical stress leads to homolytic bond dissociation, as in Figure 7(a), followed by electron transfer from the hydrocarboradicals to the more electronegative fluorocarboradicals.<sup>38</sup>

Studies using KFM and MFM show that these mechanoradicals colocalize with the charge mosaics, and the use of radical scavengers and quantum mechanical calculations at various levels of theory indicate that mechanoradicals appear to stabilize the charges of both polarities (+ and –) that form on the tribocharged surfaces.<sup>56,62,63,83</sup> Chen *et al.*<sup>12</sup> recently reviewed the use of this phenomenon as a strategy for decreasing surface charge. Doping polymers with radical scavengers (e.g., 2,2-diphenyl-1-picrylhydrazyl (DPPH), or vitamin E ( $\pm\alpha$ -tocopherol)) decreases the surface charge they develop and increases the rate at which they discharge.<sup>59</sup> Mazur and Grzybowski showed that radicals stabilize cations by the interaction of the unoccupied orbital (LUMO) of the cation ( $R^+$ ) with the half-filled (SOMO) orbital of the radical ( $R^\bullet$ ) and subsequent formation of  $[R-R]^{+\bullet}$  species.<sup>83</sup> Likewise, the radicals stabilize anions by the



interaction of the anion ( $R^-$ ) highest occupied molecular orbital (HOMO) with the  $R^\bullet$  SOMO.

#### 4 CONCLUSIONS

The similarities are remarkable among triboelectric series generated in different laboratory settings, for different modes of contact among materials, and for materials of differing levels of contamination. The formulation of a single triboelectric series that is always consistent from experiment to experiment, however, is not likely and perhaps not possible. Our current understanding of tribocharging suggests these inconsistencies arise because multiple properties or mechanisms contribute to charging. Combinations of electron transfer, ion transfer,  $H^+$  and  $OH^-$  partitioning, bond dissociation, chemical changes, and material transfer may occur simultaneously but at different rates. Such a picture may help explain how materials can switch order in triboelectric series generated after extended duration or iterations of charging.<sup>10,22</sup> For insulating materials, these processes produce a mosaic of nanoscopic patches of mechanoradical-stabilized charge of both positive and negative polarities on each surface of a tribopair. It is the relative magnitude of charge in each patch and the number of patches of each polarity that determines the net macroscopic charge traditionally observed on tribocharged electrets. These magnitudes appear to depend, in part, on the relative strain of each material, variations of which can lead to charge reversal for a tribopair or charge transfer between otherwise identical materials. Further research is needed to probe the molecular-scale changes that occur during tribocharging. Understanding the mechanisms that underlie tribocharging could lead to greater control over the production of electrets, enhanced energy harvesting by electret-based generators and self-powered sensors, novel routes to surface functionalization, and mechanically driven chemical reactions.

#### 5 ABBREVIATIONS AND ACRONYMS

ABS = acrylonitrile butadiene styrene; CPD = charge penetration depth; EPR = electron paramagnetic resonance; ESR = electron spin resonance; IR = infrared; KFM = Kelvin-probe atomic force microscopy; MFM = magnetic force microscopy; NMR = nuclear magnetic resonance; PAN = polyacrylonitrile; PC = polycarbonate; PDMS = polydimethylsiloxane; PE = polyethylene; PET = poly(ethylene terephthalate); PMMA = poly(methyl methacrylate); PP = polypropylene; PS = polystyrene; PTFE = polytetrafluoroethylene; PV2P = poly(vinyl-2-pyridine); PVA = poly(vinyl alcohol); PVAc = poly(vinyl acetate); PVDC = poly(vinylidene chloride); SS = stainless steel; XPS = X-ray photoelectron spectroscopy.

#### 6 GLOSSARY

*Charge penetration depth (CPD)*: The depth below the surface of a film in which its tribocharge is affected.

*Contact electrification*: The transfer of charge from one material to another when those materials come into contact (with or without rubbing) and are separated.

*Donor number*: The enthalpy associated with the coordination reaction of a compound with metal cations.

*Tribocharging*: Contact electrification that explicitly involves rubbing.

*Tribopair*: A pair of materials that charge via tribocharging.

#### 7 RELATED ARTICLES

Electrets; Electrochemistry: Applications in Inorganic Chemistry; Electron Transfer Reactions: Theory; Electronic Structure of Solids; Electrochemistry; Charge Transfer

#### 8 REFERENCES

1. L. S. McCarty and G. M. Whitesides, *Angew. Chem. Int. Ed.*, 2008, **47**, 2188.
2. G. M. Sessler and R. Gerhard-Multhaupt eds., *Electrets*, 3rd edition, Laplacian, Morgan Hill, 1998.
3. W. R. Harper, *Contact and Frictional Electrification*, Laplacian, Morgan Hill, 1998.
4. J. Lowell and A. C. Rose-Innes, *Adv. Phys.*, 1980, **29**, 947.
5. R. G. Horn and D. T. Smith, *Science*, 1992, **256**, 362.
6. P. Mehrani, M. Murtomaa and D. J. Lacks, *J. Electrostat.*, 2017, **87**, 64.
7. J. W. Weigl, *Angew. Chem. Int. Ed.*, 1977, **16**, 374.
8. D. M. Pai and B. E. Springett, *Rev. Mod. Phys.*, 1993, **65**, 163.
9. A. F. Diaz and R. M. Felix-Navarro, *J. Electrostat.*, 2004, **62**, 277.
10. D. N. Ferguson, *J. South Afr. Inst. Min. Met.*, 2010, **110**, 75.
11. F. Fraas, *Electrostatic Separation of Granular Materials*; U.S. Department of the Interior, Bureau of Mines, Bulletin 603, Washington, DC, 1962.
12. L. Chen, Q. Shi, Y. Sun, T. Nguyen, C. Lee and S. Soh, *Adv. Mater.*, 2018, **30**, 1802405.
13. J. A. Wiles, B. A. Grzybowski, A. Winkleman and G. M. Whitesides, *Anal. Chem.*, 2003, **75**, 4859.
14. D. F. McGonigle and C. W. Jackson, *Pest Manag. Sci.*, 2002, **58**, 374.
15. T. A. L. Burgo, F. Galembeck and G. H. Pollack, *J. Electrostat.*, 2016, **80**, 30.



16. C. H. Park, J. K. Park, H. S. Jeon and B. C. Chun, *J. Electrostat.*, 2008, **66**, 578.
17. U. G. Musa, S. D. Cezan, B. Baytekin and H. T. Baytekin, *Sci. Rep.*, 2018, **8**, 1.
18. M. Sow, D. J. Lacks and R. M. Sankaran, *J. Appl. Phys.*, 2012, **112**, 084909.
19. M. Sow, R. Widenor, A. Kumar, S. W. Lee, D. J. Lacks and R. M. Sankaran, *Angew. Chemie Int. Ed.*, 2012, **51**, 2695.
20. J. Lowell and A. R. Akande, *J. Phys. D Appl. Phys.*, 1988, **21**, 125.
21. A. L. Collins, R. S. B. Ghosh and S. J. Putterman, Triboelectrification of single crystals as a function of orientation and surface reconstruction, in Proceedings of the 2018 Electrostatics Joint Conference, 2018, pp. 1–15.
22. H. T. Baytekin, B. Baytekin, J. T. Incorvati and B. A. Grzybowski, *Angew. Chem. Int. Ed.*, 2012, **51**, 4843.
23. R. S. B. Ghosh, A. L. Collins and S. J. Putterman, Towards a single crystal triboelectric series, in Proceedings of the 2018 Electrostatics Joint Conference, 2018, pp. 1–9.
24. M. M. Apodaca, P. J. Wesson, K. J. M. Bishop, M. A. Ratner and B. A. Grzybowski, *Angew. Chem. Int. Ed.*, 2010, **49**, 946.
25. A. E. Wang, P. S. Gil, M. Holonga, Z. Yavuz, H. T. Baytekin, R. M. Sankaran and D. J. Lacks, *Phys. Rev. Mater.*, 2017, **1**.
26. J. Chen and Z. L. Wang, *Joule*, 2017, **1**, 480.
27. C. G. Camara, S. J. Putterman and A. Kotowski, *Proc. SPIE*, 2015, **9590**, 959005.
28. A. L. Collins, C. G. Camara, E. Van Cleve and S. J. Putterman, *Rev. Sci. Instrum.*, 2018, **89**.
29. G. K. Kaufman, M. Reches, S. W. Thomas, J. Feng, B. F. Shaw and G. M. Whitesides, *Appl. Phys. Lett.*, 2009, **94**, 044102.
30. G. K. Kaufman, S. W. Thomas III, M. Reches, B. F. Shaw, J. Feng and G. M. Whitesides, *Soft Matter*, 2009, **5**, 1188.
31. L. S. McCarty, A. Winkleman and G. M. Whitesides, *J. Am. Chem. Soc.*, 2007, **129**, 4075.
32. T. A. D. L. Burgo, C. A. Rezende, S. Bertazzo, A. Galembeck and F. Galembeck, *J. Electrostat.*, 2011, **69**, 401.
33. J. A. Wiles, M. Fialkowski, M. R. Radowski, G. M. Whitesides, B. A. Grzybowski and J. Phys., *Chem. B*, 2004, **108**, 20296.
34. S. W. Thomas III, S. J. Vella, G. K. Kaufman and G. M. Whitesides, *Angew. Chem. Int. Ed.*, 2008, **47**, 6654.
35. S. W. Thomas III, S. J. Vella, M. D. Dickey, G. K. Kaufman and G. M. Whitesides, *J. Am. Chem. Soc.*, 2009, **131**, 8746.
36. S. Friedle and S. W. Thomas, *Angew. Chem. Int. Ed.*, 2010, **49**, 7968.
37. H. T. Baytekin, A. Z. Patashinski, M. Branicki, B. Baytekin, S. Soh and B. A. Grzybowski, *Science*, 2011, **333**, 308.
38. T. A. L. Burgo, T. R. D. Ducati, K. R. Francisco, K. J. Clinckspoor, F. Galembeck and S. E. Galembeck, *Langmuir*, 2012, **28**, 7407.
39. D. Puhan, R. Nevshupa, J. S. S. Wong and T. Reddyhoff, *Tribol. Int.*, 2019, **130**, 366.
40. E. Yilmaz, H. Sezen and S. Suzer, *Angew. Chem. Int. Ed.*, 2012, **51**, 5488.
41. M. W. Williams, *AIP Adv.*, 2012, **2**.
42. L. Xie, G. Li, N. Bao and J. Zhou, *J. Appl. Phys.*, 2013, **113**, 184908.
43. S. Pan and Z. Zhang, *Friction*, 2019, **7**, 2.
44. D. J. Lacks and R. Mohan Sankaran, *J. Phys. D Appl. Phys.*, 2011, **44**, 453001.
45. C. X. Lu, C. B. Han, G. Q. Gu, J. Chen, Z. W. Yang, T. Jiang, C. He and Z. L. Wang, *Adv. Eng. Mater.*, 2017, **19**, 1700275.
46. Y. Su, J. Chen, Z. Wu and Y. Jiang, *Appl. Phys. Lett.*, 2015, **106**.
47. X. Wen, Y. Su, Y. Yang, H. Zhang and Z. L. Wang, *Nano Energy*, 2014, **4**, 150.
48. M. Olsen, J. Örtengren, R. Zhang, S. Reza, H. Andersson and H. Olin, *Sci. Rep.*, 2018, **8**, 5293.
49. C. Liu and A. J. Bard, *Nat. Mater.*, 2008, **7**, 505.
50. C. Liu and A. J. Bard, *J. Am. Chem. Soc.*, 2009, **131**, 6397.
51. C. Liu and A. J. Bard, *Chem. Phys. Lett.*, 2009, **480**, 145.
52. C. Liu and A. J. Bard, *Chem. Phys. Lett.*, 2010, **485**, 231.
53. S. Pan, N. Yin and Z. Zhang, *Sci. Rep.*, 2018, **8**, 2470.
54. S. Pan and Z. Zhang, *J. Appl. Phys.*, 2017, **122**, 144302.
55. L. S. McCarty, A. Winkleman and G. M. Whitesides, *Angew. Chem. Int. Ed.*, 2007, **46**, 206.
56. B. Baytekin, H. T. Baytekin and B. A. Grzybowski, *J. Am. Chem. Soc.*, 2012, **134**, 7223.
57. S. Piperno, H. Cohen, T. Bendikov, M. Lahav and I. Lubomirsky, *Phys. Chem. Chem. Phys.*, 2012, **14**, 5551.
58. S. Piperno, H. Cohen, T. Bendikov, M. Lahav and I. Lubomirsky, *Angew. Chem. Int. Ed.*, 2011, **50**, 5654.
59. H. T. Baytekin, B. Baytekin, T. M. Hermans, B. Kowalczyk and B. A. Grzybowski, *Science*, 2013, **341**, 1368.
60. R. K. Pandey, H. Kakehashi, H. Nakanishi, S. Soh and J. Phys., *Chem. C*, 2018, **122**, 16154.
61. A. R. Akande and J. Lowell, *J. Phys. D Appl. Phys.*, 1987, **20**, 565.
62. H. T. Baytekin, B. Baytekin, S. Huda, Z. Yavuz and B. A. Grzybowski, *J. Am. Chem. Soc.*, 2015, **137**, 1726.
63. C. Yun, S.-H. Lee, J. Ryu, K. Park, J.-W. Jang, J. Kwak and S. Hwang, *J. Am. Chem. Soc.*, 2018, **140**, 14687.
64. T. R. D. Ducati, L. H. Simões and F. Galembeck, *Langmuir*, 2010, **26**, 13763.
65. K. Hiratsuka and K. Hosotani, *Tribol. Int.*, 2012, **55**, 87.

66. J. Liu, J. K. Floess, H. Tu and D. V. Fomitchev, *J. Imaging Sci. Technol.*, 2012, **56**, 050403-1.
67. Y. Hiraga, Y. Teramoto, N. Miyagawa and K. Hoshino, *Langmuir*, 2013, **29**, 6903.
68. B. A. Grzybowski, M. Fialkowski and J. A. Wiles, *J. Phys. Chem. B*, 2005, **109**, 20511.
69. H. T. Baytekin, B. Baytekin, S. Soh and B. A. Grzybowski, *Angew. Chem. Int. Ed.*, 2011, **50**, 6766.
70. X. Ma, D. Zhao, M. Xue, H. Wang and T. Cao, *Angew. Chem. Int. Ed.*, 2010, **49**, 5537.
71. R. F. Gouveia, J. S. Bernardes, T. R. D. Ducati and F. Galembeck, *Anal. Chem.*, 2012, **84**, 10191.
72. W. M. Haynes ed., *CRC Handbook of Chemistry and Physics*, 93rd edition, CRC Press, Boca Raton, FL, 2012.
73. M. W. Williams, *IEEE Trans. Ind. Appl.*, 2011, **47**, 1093.
74. E. Nikitina, *J. Imaging Sci. Technol.*, 2009, **53**, 40503-1.
75. A. F. Diaz, *IBM J. Res. Dev.*, 1993, **37**, 249.
76. J. A. Medley, *Nature*, 1953, **171**, 1077.
77. A. F. Diaz, *J. Adhes.*, 1998, **67**, 111.
78. A. F. Diaz, D. Wollmann and D. Dreblow, *Chem. Mater.*, 1991, **3**, 997.
79. A. J. Alexander, *Langmuir*, 2012, **28**, 13294.
80. J. Henniker, *Nature*, 1962, **196**, 474.
81. K. Sayfidinov, S. D. Cezan, B. Baytekin and H. T. Baytekin, *Sci. Adv.*, 2018, **4**, eaau3808.
82. A. M. Barnes and A. D. Dinsmore, *J. Electrostat.*, 2016, **81**, 76.
83. T. Mazur and B. A. Grzybowski, *Chem. Sci.*, 2017, **8**, 2025.